MCB
Journals.ASM.org

A Novel Function of p38-Regulated/Activated Kinase in Endothelial Cell Migration and Tumor Angiogenesis

Naoto Yoshizuka,[a] Rebecca M. Chen,[a,b] Zeyu Xu,[a,c] Rong Liao,[a] Lixin Hong,[a] Wen-Yuan Hu,[d] Guoliang Yu,[b] Jiahuai Han,[e,f] Longchuan Chen,[g] and Peiqing Sun[a]

Departments of Molecular Biology[a] and Immunology and Microbial Science,[e] The Scripps Research Institute, La Jolla, California, USA; Epitomics, Inc., Burlingame, California, USA[b]; University of California at Irvine, Irvine, California, USA[c]; Biosettia, Inc., San Diego, California, USA[d]; State Key Laboratory of Cellular Stress Biology and School of Life Sciences, Xiamen University, Xiamen, Fujian, China[f]; and Diagnostic and Molecular Medicine Health Care Group, Veterans Affairs Medical Center, Long Beach, California, USA[g]

The p38 mitogen-activated protein kinase (MAPK) pathway has been implicated in both suppression and promotion of tumorigenesis. It remains unclear how these 2 opposite functions of p38 operate *in vivo* to impact cancer development. We previously reported that a p38 downstream kinase, p38-regulated/activated kinase (PRAK), suppresses tumor initiation and promotion by mediating oncogene-induced senescence in a murine skin carcinogenesis model. Here, using the same model, we show that once the tumors are formed, PRAK promotes the growth and progression of skin tumors. Further studies identify PRAK as a novel host factor essential for tumor angiogenesis. In response to tumor-secreted proangiogenic factors, PRAK is activated by p38 via a vascular endothelial growth factor receptor 2 (VEGFR2)-dependent mechanism in host endothelial cells, where it mediates cell migration toward tumors and incorporation of these cells into tumor vasculature, at least partly by regulating the phosphorylation and activation of focal adhesion kinase (FAK) and cytoskeletal reorganization. These findings have uncovered a novel signaling circuit essential for endothelial cell motility and tumor angiogenesis. Moreover, we demonstrate that the tumor-suppressing and tumor-promoting functions of the p38-PRAK pathway are temporally and spatially separated during cancer development *in vivo*, relying on the stimulus, and the tissue type and the stage of cancer development in which it is activated.

The p38 mitogen-activated protein kinase (MAPK) was initially identified as a major mediator of inflammatory and stress responses (35) and later found to be involved in multiple cellular processes and in diseases such as cancer (2, 16, 31). Previous studies have identified the critical role of p38 in tumor-suppressing cellular processes, including oncogene-induced senescence (6, 17, 23, 48), replicative senescence (23), contact inhibition (8, 13), and DNA damage responses (5, 18, 36, 49). The tumor-suppressing activity of the p38 pathway has been demonstrated both in cell culture and in murine cancer models (20, 45, 47). In addition, the p38 pathway has also been implicated in cancer promotion. p38 mediates migration and invasion in cultured tumor cells (19, 43), and the production of tumor-promoting cytokines such as interleukin-6 (IL-6) in stromal cells (14, 46). Several *in vitro* studies have linked p38 to tumor angiogenesis. p38 is essential for the expression of an important proangiogenic factor, vascular endothelial growth factor (VEGF), in cultured tumor cell lines (44, 51). In primary cultured human umbilical vein endothelial cells (HUVECs), p38 can be activated in response to VEGF treatment, and pharmacological inhibition of p38 attenuated VEGF-induced cell migration (38, 39). These findings suggest a requirement of p38 by either tumor cells or host endothelial cells, or both, in tumor angiogenesis. However, these studies were carried out in cultured cells, and the role of the p38 pathway in tumor angiogenesis *in vivo* has yet to be determined.

While the potential roles of p38 in tumor suppression and tumor promotion are both supported by experimental evidence, it remains unclear how these 2 opposing functions of p38 operates *in vivo* to impact cancer development. Like other MAPKs, the functions of p38 are mediated by its downstream substrates, including serine/threonine protein kinases such as p38-regulated/activated kinase (PRAK) and MAPK-activated kinases 2 (MK2) (42). We previously demonstrated that PRAK works as a tumor suppressor by mediating oncogene-induced senescence during 7,12-dimethylbenzanthracene (DMBA)-induced skin carcinogenesis (45). DMBA is a well-characterized environmental mutagen that induces skin carcinogenesis in mouse models (11). DMBA-induced skin carcinogenesis is divided into 3 stages: initiation (induction of stable oncogenic mutations, such as those activating *ras*, by DMBA), promotion (proliferation of genetically altered cells), and progression (growth of the tumors and conversion of papillomas to carcinomas) (12). While DMBA induces efficient skin tumorigenesis when combined with a chemical tumor promoter such as tetradecanoyl phorbol 13-acetate (TPA) (2-stage carcinogenesis), DMBA-alone-induced tumor formation (1-stage carcinogenesis) is poor in wild-type mice but can be enhanced in strains deficient for tumor suppressor genes. We found that PRAK deficiency compromised senescence induction and increased the incidence and reduced the latency of tumor formation induced by the 1-stage protocol, while having no effect on the incidence or latency of the 2-stage carcinogenesis (45). These results indicate that PRAK suppresses the initiation/promotion stage of skin carcinogenesis by mediating oncogene-induced senescence.

Received 19 September 2011 **Returned for modification** 14 October 2011
Accepted 15 November 2011
Published ahead of print 28 November 2011
Address correspondence to Peiqing Sun, pqsun@scripps.edu.
This article is Scripps manuscript no. 20483.

doi:10.1128/MCB.06301-11

In the current study, we uncovered a tumor promoting function of PRAK in the 2-stage skin carcinogenesis model. We demonstrate that once the skin tumors are formed in this model, PRAK can be activated in the host endothelial cells by tumor-secreted proangiogenesis factors and mediate tumor angiogenesis essential for sustained growth and malignant progression of the skin tumors. Further studies indicate that PRAK is activated by p38 and promotes the migration of host endothelial cells toward tumors, at least partly by regulating the phosphorylation and activation of focal adhesion kinase (FAK) on focal contacts and cytoskeletal reorganization. Our findings have thus revealed that the tumor-suppressing and tumor-promoting functions of the p38-PRAK pathway operate in different tissue types and at different stages of carcinogenesis, upon activation by different stimuli. Therefore, these 2 opposing functions of the p38-PRAK pathway are separated temporally and spatially during cancer development.

MATERIALS AND METHODS

Mouse and chemical carcinogenesis. The PRAK knockout allele was initially generated in the 129/Sv × C57BL/6 background (45) and then crossed into the FVB/N strain for 7 generations. Genotypes of the mice were determined by allele-specific PCR as described previously (45). The 2-step chemical carcinogenesis was performed as described previously (45). Briefly, 6- to 8-week-old mice were shaved 2 days before topical initiation on the back with 0.2 ml of acetone containing 25 μg of 7,12-dimethylbenzanthracene (DMBA; Sigma). One week after initiation, mice were promoted with 0.2 ml of acetone containing 12.5 μg of tetradecanoyl phorbol 13-acetate (TPA; Calbiochem) twice a week for 17 weeks. Tumors were monitored twice weekly for up to 60 weeks post-TPA treatment. The longest diameter of the largest tumor and the total number of tumors per mouse were recorded weekly. Statistical analysis of Kaplan-Meier tumor-free survival plots is based on the log-rank (Mantel-Cox) test. Statistical analysis of tumor sizes was performed by *t* test. Tumor tissues were snap-frozen and stored at −70°C or fixed in 10% formaldehyde–phosphate-buffered saline (PBS) and subsequently subjected to histopathological analysis. Papillomas and carcinomas were scored by their morphological appearance and histopathological findings.

Immunohistochemical (IHC) and immunofluorescent analysis. Formalin-fixed samples were deparaffinized with Toluene and rehydrated in alcohol gradients. To detect von Willebrand factor (vWF), slides were treated with 20 μg/ml of proteinase K (Roche) for 5 min at 55°C followed by 5 min at room temperature and then incubated with a rabbit anti-vWF antibody (AbCam) at 4°C overnight. To detect mouse CD31, deparaffinized slides were treated with 36 μg/ml of proteinase K (Roche) for 30 min at 37°C and then incubated with a rat anti-mouse CD31 antibody (553370; BD PharMingen) at 4°C overnight. To detect VEGF, deparaffinized sections were incubated in 10 mM citrate (pH 6.0) at subboiling temperature for 20 min to retrieve antigen and then incubated with an anti-VEGF antibody (C20; Santa Cruz). All the samples were then incubated with a biotinylated anti-rabbit (vWF and VEGF) or anti-rat (CD31) IgG antibody, and signals were detected by Vectastatin ABC kit (Vector Laboratories). Samples were counterstained with hematoxylin.

Apoptosis was determined by terminal deoxynucleotidyltransferase-mediated dUTP-biotin nick end labeling (TUNEL) assay (Chemicon) following the manufacturer's protocol.

To determine the contribution of HUVECs to angiogenesis in the Lewis lung carcinoma (LLC) xenografts, HUVEC-containing blood vessels were detected using a mouse anti-human CD31 antibody (550389; BD PharMingen). Deparaffinized formalin-fixed samples were treated with 20 μg/ml of proteinase K (Roche) for 5 min at 55°C and for additional 5 min at room temperature. After incubation with the primary antibody at 4°C overnight and at 37°C for additional 30 min, samples were incubated with a fluorescein isothiocyanate (FITC)-labeled anti-mouse IgG antibody.

To determine the purity of the mouse vascular endothelial cell (MVEC) preparations, MVECs and HUVECs were seeded at 2×10^4 cells/well on an 8-well glass slide (Lab-TekII Chamber System), fixed with 4% paraformaldehyde-PBS, stained with a rat anti-mouse CD31 antibody (MVEC) (550274; BD PharMingen) or a mouse anti-human CD31 antibody (HUVEC) (550389; BD PharMingen) and a FITC-conjugated secondary antibody, and mounted with DAPI (4′,6-diamidino-2-phenylindole)-containing medium.

Images were captured by an Axiovert fluorescence microscope and Axiovision image capture system (Carl Zeiss).

Cell culture, shRNAs, and virus-based gene transduction. HUVECs were obtained from ATCC, cultured in complete EGM2 medium (Lonza), and immortalized by hTERT-encoding recombinant retroviruses. LLC cells were obtained from ATCC and cultured in Dulbecco's modified Eagle's medium (DMEM) with 10% fetal bovine serum and 1% antibiotics. Short hairpin RNAs (shRNAs) targeting PRAK (45) and p38α (24) were described previously and introduced into HUVECs or MVECs via retroviruses as described previously (48). shRNAs for VEGF receptor 1 (VEGFR1), VEGFR2, neuropilin-1 (NRP1), NRP2, extracellular signal-regulated kinase 3 (ERK3) ERK4, and MK2 (sequences available upon request) were designed and cloned into pLV-H1-EF1α-puro based on the single-oligonucleotide RNA interference (RNAi) technology (Biosettia) and transduced into cells by following the manufacturer's protocol. The efficacy of shRNA was determined by Western blot analysis or real-time PCR. At least 2 effective shRNA constructs were selected for functional analysis for each gene to rule out off-target effects. Hygromycin B (50 μg/ml) and puromycin (2 μg/ml) were utilized to select transduced cells.

Quantitative real-time PCR analysis. RNA was isolated from cells by using TRIzol reagent and converted to cDNA with an oligo(dT) primer and Moloney murine leukemia virus (MMLV) reverse transcriptase (Life Technologies). PCR was performed in an ABI 7900 sequence detection system using the 2× SYBR green PCR master mix (Applied Biosystems) and gene-specific primers (sequences available upon request) in triplicate. The mRNA level for each gene was normalized to that of glyceraldehyde-3-phosphate dehydrogenase (GAPDH).

Establishment of primary MVECs. Abdominal great vessels were isolated aseptically from 8- to 12-week-old mice and incubated with dispase overnight at 4 C and then with 0.05% trypsin-EDTA for 10 to 15 min (50). Cells were neutralized with trypsin-neutralizing solution (TNS; Lonza), spun down, and resuspended in EGM2-MV medium (Lonza). To enrich the endothelial cell population, cells were continuously cultivated in EGM2-MV for 3 or 4 passages or until they displayed a uniform, endothelial cell morphology.

Establishment of primary skin papilloma cell culture. Primary keratinocytes from skin papillomas were established following a protocol provided by the manufacturer of defined keratinocyte serum-free medium (D-ksfm) (Life Technologies). Surgically excised tumors from skin papillomas were rinsed in cold PBS, incubated in antibiotics-antimycotics-PBS cocktail (Life Technologies) on ice for 1 h, and cut into pieces. Several pieces were fixed in 10% formaldehyde-PBS or frozen in optimal-cutting-temperature (OCT) medium (Sakura Finetek, Torrance, CA) for histology. The remaining pieces were minced by scalpel and digested with 25 units/ml of dispase (Life Technologies) with antibiotics-antimycotics cocktail overnight at 4°C with mild agitation. The tissues were incubated with 0.05% trypsin-EDTA for 10 to 15 min and then with TNS (Lonza) to terminate the digestion. Cells were cultivated in D-ksfm. The skin tumor supernatant used in migration assays was produced by incubating subconfluent primary tumor cells in a 10-cm cell culture dish with 4 ml of serum/growth factor-free basic EGM2 (Lonza) for 2 days.

***In vitro* cell migration assay.** Cell migration was determined using 24-well modified Boyden chambers (Costar) containing a polycarbonate membrane with 8.0-μm pores. The bottom surfaces of membranes were coated with 6.6 μg/ml collagen I (Upstate) for 1 h at room temperature.

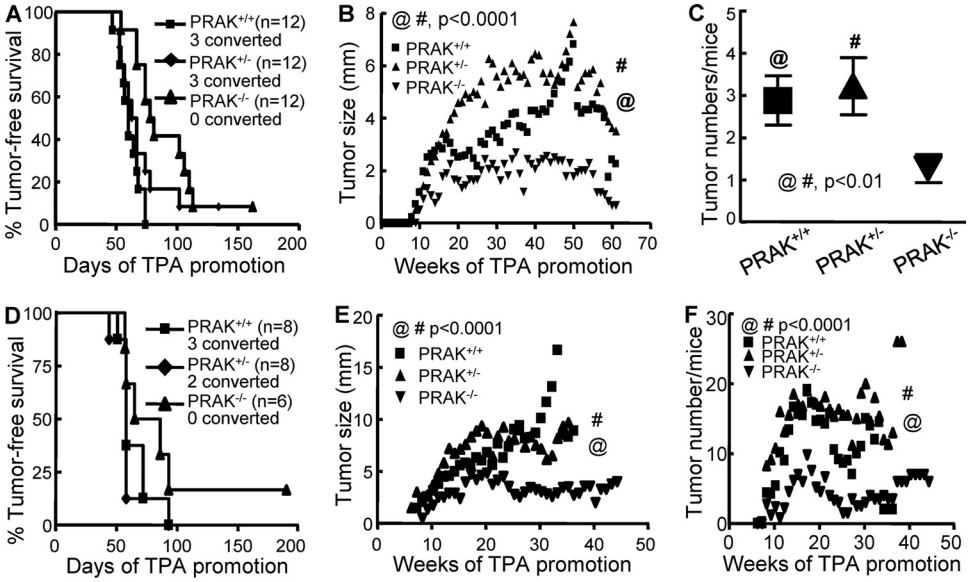

FIG 1 PRAK is essential for sustained growth and malignant progression of tumors during skin carcinogenesis. (A and D) Kaplan-Meier plots for tumor-free survival of PRAK$^{+/+}$, PRAK$^{+/-}$, and PRAK$^{-/-}$ littermates in the 129/Sv × C57BL/6 (A) or FVB/N (D) background treated with 2-stage skin carcinogenesis protocol. The number of mice with converted carcinomas is indicated. (B and E) The growth of tumors induced as described in panels A and D, respectively. The average size of the largest tumor on each mouse of the same genotype was plotted over the entire observation period (60 or 45 weeks, respectively, for panels B and E, after the initial TPA promotion). Statistical significance ($P < 0.0001$) for PRAK$^{+/+}$ versus PRAK$^{-/-}$ (@) and PRAK$^{+/-}$ versus PRAK$^{-/-}$ (#) was examined by unpaired *t* test. (C and F) Average number of tumors/mouse at the termination of observation in the study shown in panel A or over the entire observation period in the study shown in panel B, respectively. Statistical significance for PRAK$^{+/+}$ versus PRAK$^{-/-}$ (@) and PRAK$^{+/-}$ versus PRAK$^{-/-}$ (#) was examined by unpaired *t* test.

HUVECs were starved in serum/growth factor-free basic EGM2 overnight at 37°C before being harvested with trypsin. After neutralizing and removing trypsin, cells were resuspended in serum/growth factor-free EGM2, incubated for 1 h at room temperature, and seeded at 1×10^4 cells/well in the upper chamber. Five hundred microliters of serum/growth factor-free basic EGM2, skin tumor supernatant, or serum/growth factor-free EGM2 with 20 ng/ml of VEGF was added to the bottom chamber as chemoattractants. After incubation for 24 h at 37°C, cells on the upper surface of membrane were removed by cotton swabs, and the number of migrated cells on the bottom surface was counted under microscope (10 fields per filter) after staining with Giemsa (Sigma). To neutralize VEGF, tumor supernatant, medium containing recombinant VEGF, or control medium was preincubated with 10 μg/ml of an anti-VEGF antibody (C-1) (Santa Cruz) or an antiactin antibody (Sigma) (as the negative control) overnight at 4°C with mild agitation before being added to the Boyden chambers as the chemoattractant. In some experiments, 10 μM SB203580, 25 μM PD98053, 5 μM U0126, or dimethyl sulfoxide (DMSO) was added to the Boyden chambers to inhibit the relevant MAPKs.

Western blotting. Cell lysates were prepared in radioimmunoprecipitation assay (RIPA) buffer (10 mM Tris, pH 8.0, 140 mM NaCl, 1% Triton X-100, 1% sodium deoxycholate, and 0.1% sodium dodecyl sulfate) with complete protease inhibitor cocktail (Roche), 1 mM sodium orthovanadate, 10 mM sodium fluoride, and 1 mM β-glycerophosphate. Cleared cell lysates were subjected to SDS-PAGE using 6, 8, or 10% polyacrylamide gel and transferred to nitrocellulose membranes. The primary antibodies were from Cell Signaling (p38-pT180Y182, ERK-pT202Y204, ERK2, ERK3, heat shock protein 27 [HSP27]-pS82, HSP27, and MK2), BD Bioscience (FAK-pY397 and FAK), Epitomics (ERK4, VEGFR1, VEGFR2, and NRP2), Abgent (NRP1), or Sigma (actin). The antibodies against PRAK (45), p38α, and p38β (24) was described previously. The rabbit monoclonal anti-PRAK-pT182 antibody was raised in Epitomics (Burlingame, CA).

Immunoprecipitation-coupled protein kinase assay. Fifty percent confluent HUVECs were starved in serum/growth factor-free basic EGM2 overnight before treated with tumor supernatant or 20 ng/ml VEGF for the indicated time. Sometimes, cells were pretreated with 10 μM SB203580, 25 μM PD98053, or DMSO for 2.5 h. Cells were then lysed in buffer containing 50 mM HEPES, pH 7.5, 2.5 mM EGTA, 1 mM EDTA, 1% Triton X-100, 150 mM NaCl, 10% glycerol, 1 mM phenylmethylsulfonyl fluoride (PMSF), 50 mM NaF, 1 mM sodium vanadate, 1 mM β-glycerophosphate, 1 mM dithiothreitol (DTT), and complete protease inhibitors. Lysate (400 [or 200] μg) was incubated with 4 (or 2.5) μl of an antibody against PRAK, MK2, p38α, or p38β in a 300-μl (or 200-μl) volume at 4°C for 2 h, followed by incubation with 20 μl (bead volume) of Protein A Sepharose CL-4B at 4°C for 2 h. The beads were washed with lysis buffer and kinase buffer (50 mM HEPES, pH 7.5, 0.5 mM EGTA, 10 mM $MgCl_2$, 0.1 mM PMSF, 1 mM NaF, 0.1 mM sodium vanadate, 0.1 mM β-glycerophosphate, and 1 mM DTT). Kinase reactions were performed in 20 μl of 1× kinase buffer (above) with 10 μM ATP, 0.5 μl of [γ-^{32}P]ATP and 5 to 10 μg of HSP27 (for PRAK and MK2) or glutathione *S*-transferase (GST)-ATF2 (for p38α or p38β) at 30°C for 45 min, stopped by 7 μl of 4× Laemmli buffer, heated at 95°C, and separated by SDS-PAGE. Radioactive signals were detected by a phosphorimager.

Analysis of LLC/HUVEC xenograft tumor model. LLCs and HUVECs were cotransplanted as described previously (10). LLC cells (5×10^5) and HUVECs (5×10^5) were mixed in 200 μl of growth factor-reduced Matrigel (BD Bioscience) and injected subcutaneously into the athymic nu/nu mice. Tumor size was measured 3, 5, 7, 10, and 12 days after transplantation. The tumor volume was calculated using the formula length × width^2/2 and statistically analyzed by two-way analysis of variance (ANOVA) test.

Analysis of the syngeneic xenograft model. Primary skin tumor cells (1×10^6) isolated from FVB/N PRAK$^{+/+}$ papilloma were injected subcutaneously into FVB/N PRAK$^{+/+}$, PRAK$^{+/-}$, and PRAK$^{-/-}$ littermates (12 mice/genotype). Tumor size was measured 2 weeks after transplantation and statistically analyzed by *t* test.

Detection of proangiogenic cytokines secreted by skin tumors. Proangiogenic factors present in skin tumor supernatant was determined

in mouse angiogenesis enzyme-linked immunosorbent assay (ELISA) strip (Signosis, Inc) for tumor necrosis factor alpha (TNF-α), insulin-like growth factor 1 (IGF-1), VEGF, IL-6, basic fibroblast growth factor (FGF), gamma interferon (IFN-γ), EGF, and platelet-derived growth factor BB (PDGF-BB) following the manufacturer's protocol. The amount of secreted cytokines was determined by optical density at 450 nm.

Analysis of actin reorganization and focal contacts. HUVECs (1×10^4) were grown on 25-mm-diameter coverslips (VWR) coated with poly-L-lysine (Sigma) overnight. Cells were starved by serum/growth factor-free basic EGM2 overnight and then treated with tumor supernatant or 20 ng/ml of VEGF for the indicated time. After fixation in 4% paraformaldehyde-PBS and permeabilization in 0.1% Triton X-100–PBS, cells were incubated sequentially with an antibody against phospho-FAK (Y397), FAK (BD Transduction Laboratories), or vinculin (Sigma); FITC-labeled secondary antibody (Santa Cruz); and rhodamine-conjugated phalloidin (Molecular Probes). Samples were mounted with DAPI-containing medium and visualized by an Axiovert fluorescence microscope.

RESULTS

PRAK is required for sustained growth and malignant conversion of DMBA-induced skin papillomas. Our previous study, focused on the initiation and promotion stages of skin carcinogenesis, revealed that PRAK works as a tumor suppressor by mediating oncogene-induced senescence during DMBA-induced skin carcinogenesis (45). To explore the *in vivo* function of PRAK in the progression stage of skin carcinogenesis, we treated wild-type and PRAK-deficient mice with the 2-stage protocol and monitored tumor induction for a prolonged period. Confirming previous findings, the 2-stage protocol efficiently induced the appearance of skin tumors in all mice. No obvious difference was observed in the incidence or latency of tumor induction among 3 PRAK genotypes (Fig. 1A). However, to our surprise, once the tumors had appeared, tumor growth was drastically impaired in the PRAK$^{-/-}$ background (Fig. 1B). The papilloma-to-carcinoma conversion rate, as determined by the morphological and histological criteria, was also reduced from 25% (3/12) in PRAK$^{+/+}$ and PRAK$^{+/-}$ mice to none in PRAK$^{-/-}$ mice (Fig. 1A). In addition to the apparent difference in tumor sizes, the average number of papillomas per PRAK$^{-/-}$ mouse was also significantly fewer than that in the other two genotypes by the end of the observation (Fig. 1C).

A similar analysis was performed in mice with the FVB/N background, which are more susceptible to DMBA-induced skin carcinogenesis. Again, although the incidences and latencies of tumor induction by the 2-stage protocol were similar among the 3 genotypes (Fig. 1D), the tumor growth rate (Fig. 1E), the average number of tumors/mouse during tumor progression stage (Fig. 1F), and the papilloma-to-carcinoma conversion rate (Fig. 1D) were greatly decreased in PRAK$^{-/-}$ mice as compared with their PRAK$^{+/+}$ and PRAK$^{+/-}$ littermates. Taken together, our findings indicate that while PRAK suppresses the tumor initiation/promotion stage, it promotes the tumor growth/progression stage of DMBA-induced skin carcinogenesis.

PRAK is essential for angiogenesis in the surrounding of skin tumors. The requirement of PRAK for skin tumor progression prompted us to examine the role of PRAK in tumor angiogenesis, which is essential for sustained tumor growth. We analyzed the formation of tumor vasculature by immunohistochemical (IHC) staining of von Willebrand factor (vWF), a blood vessel marker, and CD31, an endothelial marker. In carcinomas from either PRAK$^{+/+}$ or PRAK$^{+/-}$ mice, well-developed blood vessels were detected inside the tumor regions, mingled with tumor cells (data not shown). In unconverted papillomas, blood vessels were absent from the tumor region (the squamous epithelial layer) (Fig. 2A and B). However, abundant vWF- and CD31-positive blood vessels were detected in the subcutaneous connective tissue layers near the tumor epithelium in the papillomas from PRAK$^{+/+}$ (Fig. 2Aa, Ad, Bg, and Bh) or PRAK$^{+/-}$ (Fig. 2Ab and Ae) mice of either 129/Sv × C57BL/6 (Fig. 2Aa, Ab, Ad, and Ae) or FVB/N (Fig. 2Bg and Bh) background. These blood vessels existed either between the tumor epithelial layers (Fig. 2Aa, Ab, and Bg) or in the stromal regions immediately below the papillomas (Fig. 2Ad, Ae, and Bh). In contrast, in PRAK$^{-/-}$, papillomas of sizes similar to the PRAK$^{+/+}$ and PRAK$^{+/-}$ tumors (about 3 to 4 mm in diameter), a much lower quantity of blood vessels was present in the subcutaneous tissues immediately below the tumor epithelium (Fig. 2Af, Bj, and C, bottom) and essentially none in the folds between squamous epithelia (Fig. 2Ac, Bi, and C, top) in either the 129/Sv × C57BL/6 (Fig. 2Ac and Af) or the FVB/N (Fig. 2Bi and Bj) background. The same observations were made in tumors that differed in size but were derived from mice after the same period of TPA promotion (data not shown). Thus, angiogenesis in regions surrounding the skin papillomas is impaired in PRAK$^{-/-}$ animals.

Inversely correlating with the formation of tumor vasculature, the number of TUNEL-positive apoptotic cells was greatly increased in the PRAK$^{-/-}$ tumor epithelia (Fig. 2Dm and Dp) as compared with the wild-type and PRAK$^{+/-}$ tumors (Fig. 2Dk, Dl, Dn, and Do) in both 129/Sv × C57BL/6 (Fig. 2Dk, Dl, and Dm) and FVB/N (Fig. 2Dn, Do, and Dp) backgrounds. This suggests that impaired angiogenesis in PRAK-null mice leads to inadequate blood supply to tumors and deprives tumors of oxygen and nutrients, resulting in increased apoptosis in tumor epithelia and attenuated tumor growth.

PRAK is required by the host endothelial cells for tumor growth and tumor angiogenesis. Tumor angiogenesis requires the migration of host endothelial cells toward tumor-secreted proangiogenic factors such as VEGF (7). Although p38 was reported essential for VEGF expression in cultured tumor cells (44, 51), IHC analysis revealed high levels of VEGF in the squamous epithelium of PRAK$^{+/+}$, PRAK$^{+/-}$, and PRAK$^{-/-}$ tumors (data not shown), indicating that PRAK is not required for VEGF production during skin carcinogenesis. We next pursued the possibility that PRAK is an essential host factor mediating tumor angiogenesis using a syngeneic xenograft model. Primary skin papilloma cells derived from wild-type FVB/N mice were subcutaneously implanted into immunocompetent, syngeneic FVB/N mice of PRAK$^{+/+}$, PRAK$^{+/-}$, or PRAK$^{-/-}$ genotype. The growth rate of the tumors transplanted into PRAK$^{-/-}$ hosts was greatly reduced as compared to those in the PRAK$^{+/+}$ and PRAK$^{+/-}$ hosts (Fig. 3A). Tumors formed in PRAK$^{+/+}$ and PRAK$^{+/-}$ mice were pink in color, while those in PRAK$^{-/-}$ mice appeared to be pale (data not shown), suggesting that the later might have contained fewer blood vessels. IHC analysis verified that tumors from the PRAK$^{+/+}$ and PRAK$^{+/-}$ hosts contained plenty of vWF-positive, mature vessels, while fewer and thinner vessels were detected in tumors from PRAK$^{-/-}$ hosts (Fig. 3B and C). Consistent with the lack

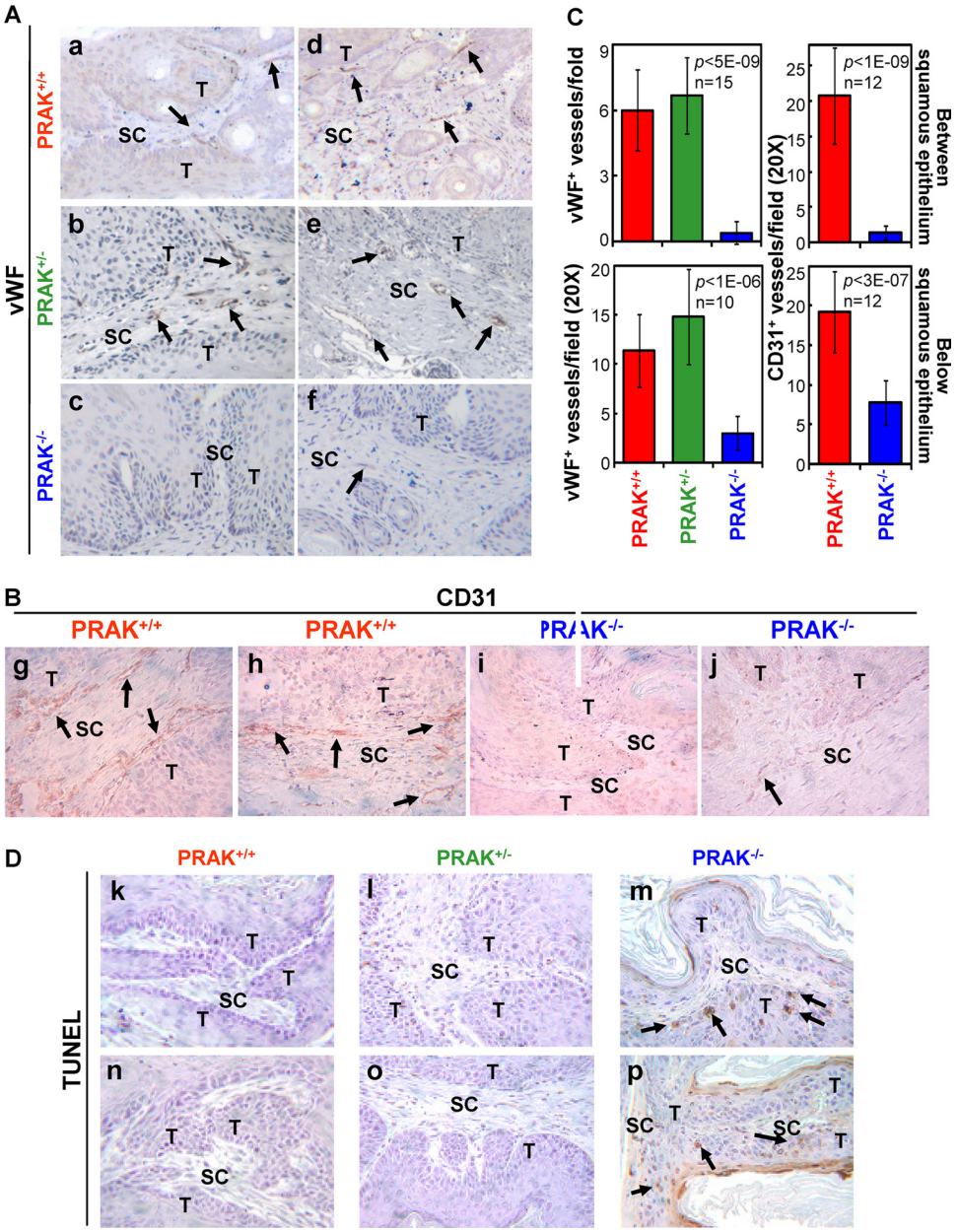

FIG 2 PRAK is essential for tumor angiogenesis during skin carcinogenesis. (A, B, and D) Immunohistochemical staining of vWF$^+$ (A), CD31$^+$ (B), and TUNEL$^+$ (D) cells in tumors induced by the 2-stage protocol in PRAK$^{+/+}$ (a, d, g, h, k, and n), PRAK$^{+/-}$ (b, e, l, and o), and PRAK$^{-/-}$ (c, f, i, j, m, and p) littermates with 129/Sv × C57BL/6 (a to f and k to m) or FVB/N (g to j and n to p) background. T, tumor epithelium; SC, subcutaneous connective tissue. Positive signals are indicated with arrowheads. (C) vWF$^+$ (left) and CD31$^+$ (right) blood vessels between (top) or immediately below (bottom) squamous epithelia were counted in 10 to 15 randomly chosen 20× fields from 4 mice/indicated genotype. Numbers are mean ± standard deviation (SD). Statistical significance was examined by unpaired *t* test.

of blood supply, apoptotic cells greatly increased in tumors from the PRAK$^{-/-}$ mice as compared to those from the PRAK$^{+/+}$ and PRAK$^{+/-}$ animals (Fig. 3D). These experiments in immunocompetent mice have revealed the requirement of PRAK in the host tumor microenvironment for tumor-induced angiogenesis and tumor growth *in vivo*.

To further investigate whether PRAK acts in the host endothelial cells to mediate tumor angiogenesis, we used a tumor/endothelial cell cotransplantation model (4, 10). Lewis lung carcinoma (LLC) cells and human umbilical vein endothelial cells (HUVECs) were mixed with Matrigel and implanted into immunocompromised nude mice. Within the first 10 days postinjection, the growth rate of the LLC tumors cotransplanted with control HUVECs was significantly enhanced as compared to when LLC cells and Matrigel were injected alone; however, this enhancement was abolished when PRAK was knocked down in HUVECs by short hairpin RNA (shRNA) (Fig. 4A). The increase in tumor growth by the control HUVECs was accompanied by incorporation of the implanted HUVECs into the vasculature of xenograft tumors, as detected

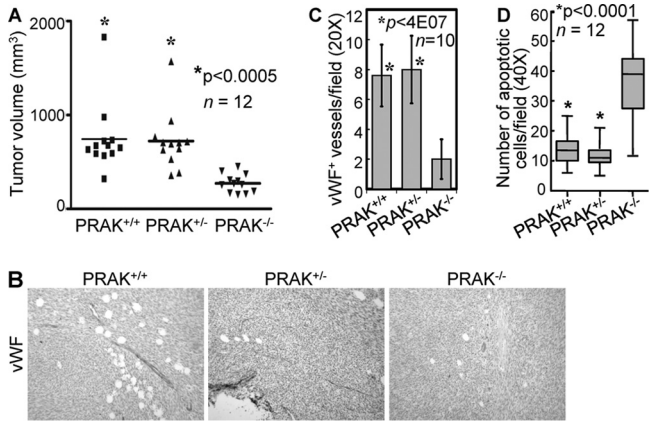

FIG 3 PRAK is a host factor required for tumor growth and tumor angiogenesis *in vivo*. (A) Scatter plots for tumor xenograft volumes 2 weeks after transplantation of skin tumor cells derived from a DMBA-TPA-treated wild-type FVB/N mouse into the syngeneic FVB/N hosts with indicated PRAK genotypes. The transverse line indicates the mean volume of 12 xenografts from mice of each genotype. ∗ indicates statistical significance for tumors from the PRAK$^{+/+}$ or PRAK$^{+/-}$ hosts versus PRAK$^{-/-}$ hosts by unpaired *t* test. (B) Immunohistochemical staining of vWF-positive cells in tumor xenografts formed by skin tumor cells in syngeneic hosts with indicated genotypes. (C) vWF^{+} vessels were counted in 10 randomly chosen 20× fields from 3 mice/indicated genotype. Numbers are mean ± SD. Statistical significance for PRAK$^{+/+}$ or PRAK$^{+/-}$ versus PRAK$^{-/-}$ was examined by unpaired *t* test. (D) Box-and-whisker plot of average number of TUNEL-positive cells in 10 randomly chosen fields (40×) per specimen in tumor xenografts formed by skin tumor cells in syngeneic hosts with indicated genotypes. Twelve mice/genotype were analyzed. ∗ indicates statistical significance for tumors from the PRAK$^{+/+}$ or PRAK$^{+/-}$ hosts versus PRAK$^{-/-}$ hosts by unpaired *t* test.

by immunofluorescence staining with an antibody specific for human CD31 (Fig. 4B). In contrast, correlating with the loss of ability to enhance tumor growth, essentially all the HUVECs with PRAK knockdown existed as single cells or clumps of a few cells without incorporation into tumor vessels (Fig. 4B). It is noted that enhanced tumor growth by HUVECs was limited to the initial 10 days postinjection, when host blood vessels (detected by IHC with an antibody specific for mouse CD31) were scarce in transplanted tumors (Fig. 4c, day 7). Beyond day 10, angiogenesis in tumors was dominated by host endothelial vessels (Fig. 4C, day 12), and the growth advantage of the tumors cotransplanted with control HUVECs was lost over those with no HUVECs or PRAK-defective HUVECs (note the curve slopes between day 10 and day 12), although the absolute sizes of the control HUVEC-LLC tumors were still the largest (Fig. 4A). Thus, in the initial period when tumor angiogenesis mainly relied on the cotransplanted HUVECs without significant contribution from the host endothelial vessels, tumor growth was stimulated by the control HUVECs but not the PRAK-defective HUVECs that failed to incorporate into tumor blood vessels. These results clearly demonstrate a requirement of PRAK by HUVECs for their incorporation into vessels and a PRAK-dependent, tumor-stimulatory role of the coinjected HUVECs.

PRAK mediates migration of endothelial cells toward tumor-secreted proangiogenic factors. Directional migration of endothelial cells is a crucial step toward the organized formation of blood vessel sprouts during angiogenesis. The re-

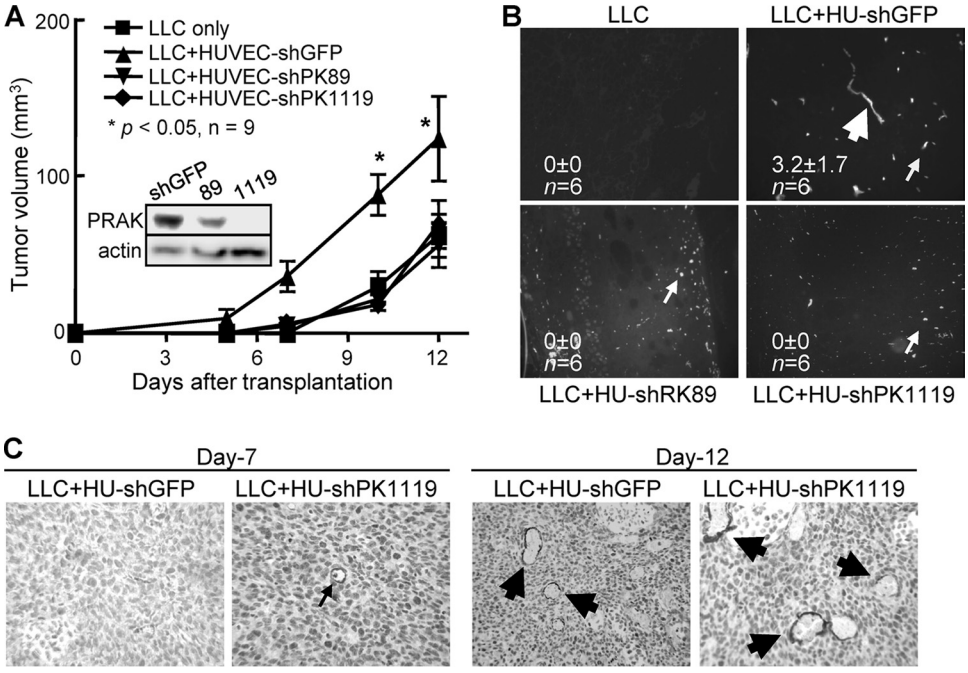

FIG 4 PRAK is required by the host endothelial cells for tumor growth and angiogenesis *in vivo*. (A) The growth of tumor xenografts formed in athymic nude mice after transplantation of LLC cells and Matrigel, in the absence (LLC only) or presence of HUVECs expressing shRNA for GFP (LLC+HU-shGFP) or PRAK (LLC+HU-shPK89 and -shPK1119). Numbers are mean tumor volume ± SD. ∗ indicates statistical significance for LLC+HU-shGFP versus the other conditions by two-way ANOVA test. (Inset) Western blot analysis demonstrating PRAK knockdown by shRNA in HUVECs. (B) Immunofluorescent staining of the transplanted HUVECs by a human-specific anti-CD31 antibody in tumor xenografts generated as described in panel A. Symbols: thick arrow, HUVEC-containing vessels; thin arrow, unincorporated HUVECs. Numbers are average numbers of human CD31^{+} vessels/field (in 6 randomly chosen 10× fields from 2 tumors) ± SD. (C) Immunohistochemical staining of tumor xenografts formed as described in panel A on day 7 or 12 postinjection, using an anti-mouse CD31 antibody.

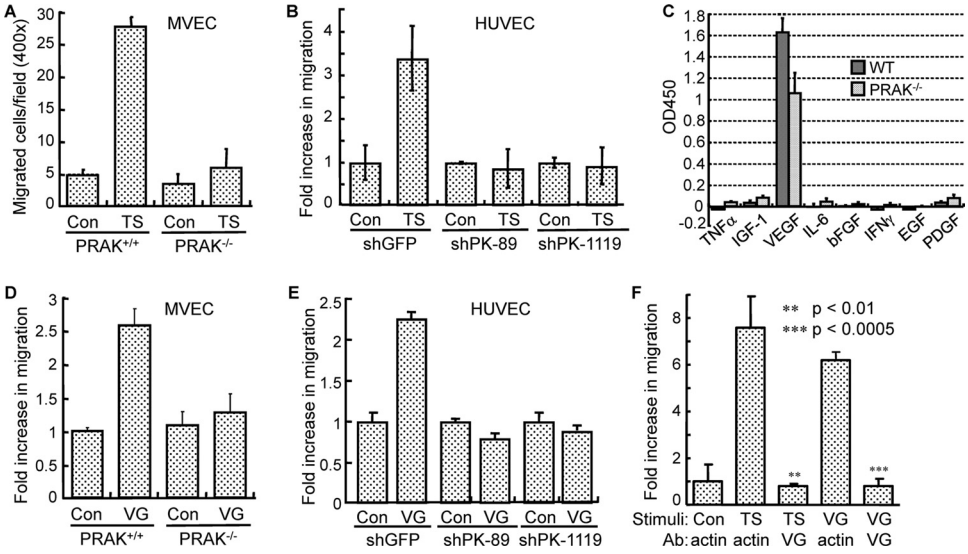

FIG 5 PRAK is required for the migration of endothelial cells induced by tumor-secreted VEGF. (A) Migration of MVECs derived from $PRAK^{+/+}$ or $PRAK^{-/-}$ littermates toward skin tumor supernatant (TS) or control medium (Con). Numbers are average numbers of cells on the bottom surfaces of membranes in 10 randomly chosen 40× fields ± SD for triplicates. (B) Migration of HUVECs transduced with shRNA for GFP (shGFP) or PRAK (shPK-89 and -1119) toward skin tumor supernatant (TS) or control medium (Con). (C) Quantification of proangiogenic cytokines in supernatants collected from $PRAK^{+/+}$ (wild type [WT]) or $PRAK^{-/-}$ skin tumor cells by ELISA. (D and E) Migration of $PRAK^{+/+}$ or $PRAK^{-/-}$ MVECs (D) or HUVECs transduced with shRNA for GFP (shGFP) or PRAK (shPK-89 and -1119) (E) toward VEGF (VG) or vehicle control (Con). (F) Neutralization of VEGF in the skin tumor supernatant abolishes endothelial cell migration. Migration of HUVECs toward control medium (Con), skin tumor supernatant (TS), or VEGF (VG) after incubation with an anti-VEGF (VG) or antiactin (actin) antibody (Ab). ** and *** indicate statistical significance for TS plus VG versus TS plus actin and VG plus VG versus VG plus actin, respectively, by unpaired *t* test. (B, D, E, and F) The number of cells having migrated to the bottom surface of membrane among 1×10^4 seeded cells was counted in 10 randomly chosen 40× fields. The fold increase in migration was calculated for each cell line by dividing the average number of cells/field in the presence of TS or VG by that without stimuli (Con). (A to F) All the numbers are mean ± SD for triplicates.

quirement of PRAK by the host endothelial cells in tumor angiogenesis raises a possibility that PRAK may mediate endothelial cell migration in response to proangiogenic factors secreted by tumors. We thus isolated primary mouse vascular endothelial cells (MVECs) from wild-type and $PRAK^{-/-}$ littermates. The MVEC preparations contained >70% of endothelial cells, based on cell surface expression of CD31 (data not shown). The tumor supernatant harvested from $PRAK^{+/+}$ skin papilloma cells induced the migration of MVECs isolated from wild-type mice but not those from $PRAK^{-/-}$ mice (Fig. 5A). Confirming this observation, human endothelial cells (HUVECs) transduced with a control shRNA, but not those with PRAK shRNA (Fig. 4A, insert), showed increased migration toward skin tumor supernatant (Fig. 5B). Neither the skin tumor supernatant nor PRAK shRNA altered the proliferation of HUVECs (data not shown), indicating that the difference in cell migration was not due to the effects on cell proliferation. These results demonstrate that PRAK is essential for migration of host endothelial toward factors secreted by the skin tumor epithelium.

To identify the migration-inducing factors secreted by skin tumors, we examined the proangiogenic factors present in the tumor supernatants by using ELISA. Among the proangiogenic factors surveyed, only VEGF was present in significant quantity in the supernatants collected from either wild-type or $PRAK^{-/-}$ papilloma cells (Fig. 5C), suggesting that VEGF is the major proangiogenic factor secreted by the skin tumors. When used as a chemoattractant, recombinant VEGF induced migration of $PRAK^{+/+}$ MVECs and HUVECs transduced with a control shRNA, but not $PRAK^{-/-}$ MVECs or HUVECs with PRAK knockdown (Fig. 5D and E). Furthermore, endothelial cell migration induced by the skin tumor supernatant was abolished by an anti-VEGF neutralizing antibody but not by an antiactin antibody (Fig. 5F), indicating that the ability of skin tumor supernatant to induce migration relies mainly on VEGF. Confirming the potency of the VEGF-neutralizing antibody, it also inhibited HUVEC migration induced by recombinant VEGF (Fig. 5F). These data demonstrate that VEGF is the major proangiogenesis factor secreted by skin tumors to induce the PRAK-dependent host endothelial cell migration, although contribution from additional factors cannot be completely ruled out. Notably, both wild-type and $PRAK^{-/-}$ skin tumors secreted comparable levels of VEGF (Fig. 5C). This is consistent with results from the IHC analysis on VEGF expression in skin tumors (data not shown) and supports the notion that PRAK deficiency impairs skin tumor angiogenesis by causing a defect in host endothelial cells rather than skin tumors.

PRAK is activated by p38, but not ERK1/2, ERK3, or ERK4, in response to tumor-secreted factors during endothelial cell migration. In addition to being a substrate for p38 (33, 45), PRAK is also a substrate for ERK1/2 (34) and atypical MAPKs ERK3 and ERK4 (40, 41). To gain insights into the signaling pathway that mediates the role of PRAK in migrating endothelial cells, we determined the contribution of p38 and ERKs to PRAK activation by examining the phosphorylation of PRAK at Thr182, a residue essential for activation (32, 33), and the protein kinase activity of PRAK immunoprecipitated from cells. Confirming the specificity of these assays, PRAK-T182 phosphorylation as detected by a

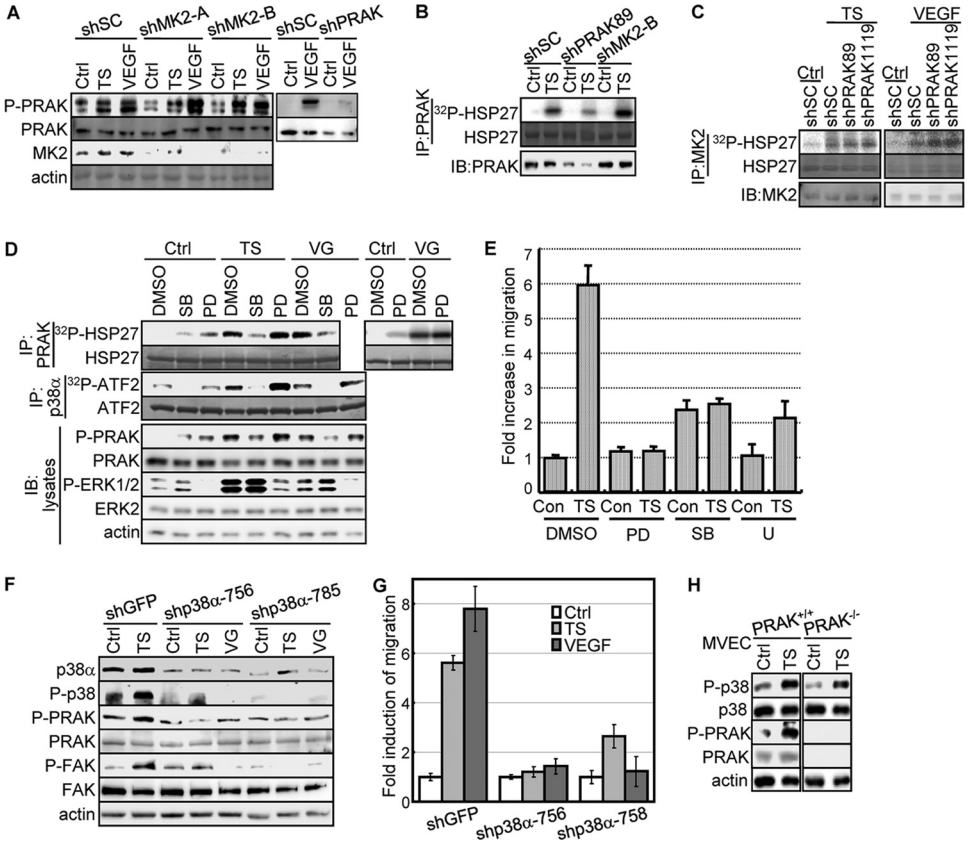

FIG 6 PRAK is activated by p38 in response to skin tumor-secreted proangiogenic factors. (A) The phospho-specific antibody against PRAK-T182 specifically recognizes activated PRAK but not MK2. Western blot analysis of HUVECs transduced with scramble shRNA (shSC) or shRNA for MK2 (shMK2-A and -B) or PRAK (shPRAK-89) and treated with the control medium (Ctrl), skin tumor supernatant (TS), or 20 ng/ml of VEGF for 30 min. (B) The HSP27 kinase activity of the immunocomplex isolated by the anti-PRAK antibody is specifically associated with PRAK, but not MK2. PRAK was immunoprecipitated from HUVECs transduced with scramble shRNA (shSC) or shRNA for PRAK (shPRAK89) or MK2 (shMK2-B) and treated with the control medium (Ctrl) or skin tumor supernatant (TS) for 30 min, using the anti-PRAK antibody, and assayed for protein kinase activity toward HSP27 in the presence of [γ-^{32}P]ATP. IB, immunoblot. (C) The HSP27 kinase activity of the immunocomplex isolated by the anti-MK2 antibody is specifically associated with MK2 but not PRAK. MK2 was immunoprecipitated from HUVECs transduced with scramble shRNA (shSC) or shRNA for PRAK (shPRAK89 and shPRAK1119) and treated with the control medium (Ctrl), skin tumor supernatant (TS), or 20 ng/ml of VEGF for 30 min, using the anti-MK2 antibody, and assayed for protein kinase activity toward HSP27 in the presence of [γ-^{32}P]ATP. (D) PRAK and p38α were immunoprecipitated (IP) by an anti-PRAK and an anti-p38α antibody, respectively, from HUVECs pretreated with DMSO, SB203580 (SB), or PD98053 (PD) and then treated with control medium (Ctrl), tumor supernatant (TS), or VEGF (VG) for 30 min, and assayed for HSP27- and ATF2-kinase activity, respectively, in the presence of [γ-^{32}P]ATP. Part of the lysates were subjected to Western blot analysis (IB:lysates). (E) Migration of HUVECs toward skin tumor supernatant (TS) or control medium (Con) in the presence of 10 μM SB203580 (SB), 25 μM PD98053 (PD), 5 μM U0126 (U), or DMSO. The fold increase in migration was calculated by dividing the average number of cells/field by that in the presence of control medium and DMSO (Con plus DMSO). (F) Western blot analysis of HUVECs transduced with shRNA for GFP (shGFP) or p38α (shp38α-756 and -785) and treated with control medium (Ctrl), tumor supernatant (TS), or VEGF (VG) for 30 min. (G) Migration of HUVECs transduced with shRNA for GFP (shGFP) or p38α (shp38α-756 and -785) toward control medium (Ctrl), tumor supernatant (TS), or VEGF (VG). The fold increase in migration was calculated for each cell line by dividing the average number of cells/field in the presence of TS or VG by that without stimuli (Con). (E and G) The number of cells on the bottom surface of the membrane among 1×10^4 seeded cells was counted in 10 randomly chosen 40× fields. All the numbers are mean ± SD for triplicates. (H) PRAK and p38 are activated by the skin tumor supernatant in MVECs. Western blot analysis of lysates from PRAK$^{+/+}$ and PRAK$^{-/-}$ MVECs treated with the control medium (Ctrl) or skin tumor supernatant (TS) for 30 min.

phospho-specific antibody and the HSP27 kinase activity of immunoprecipitated PRAK were reduced only by PRAK shRNA and not by shRNA for MK2, another PRAK-related, p38 downstream protein kinase (Fig. 6A to C).

Treatment of HUVECs with skin tumor supernatant or VEGF stimulated the kinase activity of PRAK and induced PRAK-T182 phosphorylation (Fig. 6D). The tumor supernatant and VEGF also induced the kinase activity and activating phosphorylation of p38α and p38β (Fig. 6A and data not shown), consistent with previous reports that p38 is activated by VEGF (9, 25, 38, 39). Both tumor supernatant and VEGF also activated ERK1/2 in HUVECs (Fig. 6A). Activation of PRAK and p38 by the skin tumor supernatant was also observed in primary MVECs (Fig. 6H). Thus, PRAK and p38 are activated concurrently in endothelial cells in response to tumor-secreted factors. Interestingly, the activity of p38 was induced rapidly after only 15 min of treatments and returned to the basal level after 3 h, while the activation of PRAK, albeit also rapid, persisted at least after 3 h (data not shown). These data suggest that transient activation of p38 by tumor-secreted factors leads to a more prolonged activation of its downstream kinase PRAK in migrating endothelial cells.

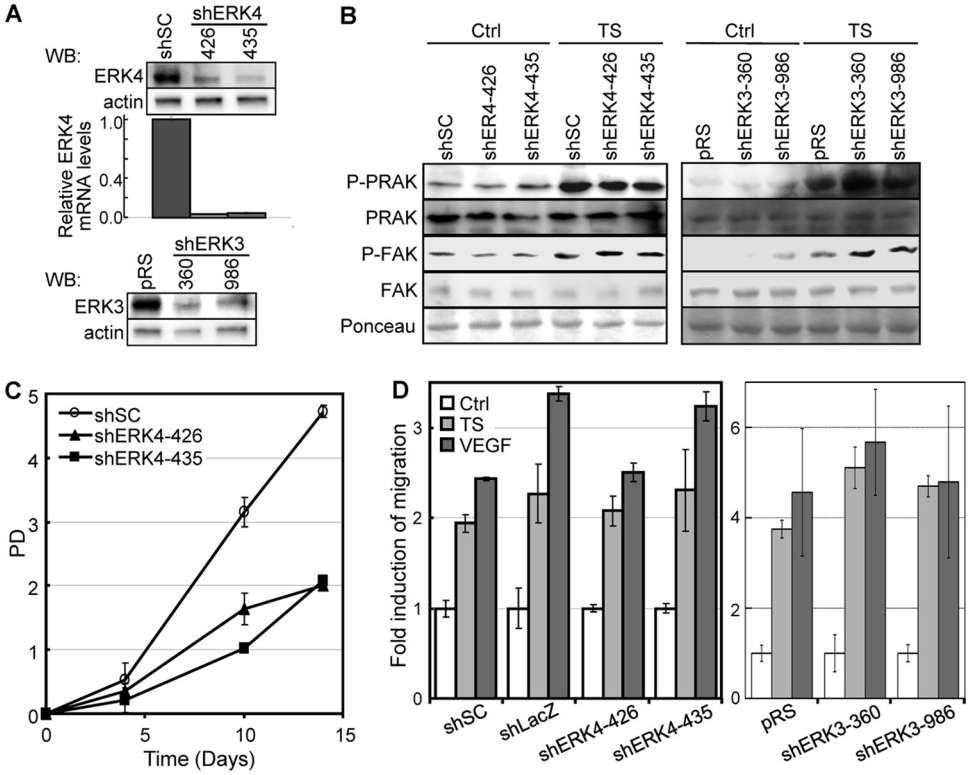

FIG 7 ERK3 and ERK4 are dispensable for the activation of PRAK and FAK and cell migration induced by skin tumor-secreted proangiogenic factors in endothelial cells. (A) Western blot (WB) (top and bottom) and quantitative real-time PCR (bar graph) analyses of HUVECs transduced with a scrambled shRNA (shSC) or shRNA for ERK4 (shERK4-426 and -435) or ERK3 (shERK3-360 and -986), showing knockdown of ERK4 and ERK3. (B) Western blot analysis of HUVECs transduced with a scrambled shRNA (shSC) or shRNA for ERK4 (shERK4-426 and -435) or ERK3 (shERK3-360 and -986) and treated with control medium (Ctrl) or skin tumor supernatant (TS) for 30 min, detecting indicated proteins. (C) Proliferation (population doubling) of HUVECs transduced with a scrambled shRNA (shSC) or shRNA for ERK4 (shERK4-426 and -435) over a period of 14 days. (D) Migration activity of HUVECs transduced with a scrambled shRNA (shSC) or shRNA for LacZ (shLacZ), ERK4 (shERK4-426 and -435), or ERK3 (shERK3-360 and -986) in response to control medium (Ctrl), skin tumor supernatant (TS), or 20 ng/ml of recombinant VEGF was measured in the Boyden chamber assay. The number of cells that had migrated to the bottom surface of the membrane among 1×10^4 seeded cells was counted in 10 randomly chosen 40× fields. The fold increase in migration was calculated for each cell line by dividing the average number of cells/field in the presence of TS or VEGF by that without stimuli (Ctrl). (A, C, and D) All the numbers are mean ± SD for triplicates.

To investigate the contribution of p38 and ERKs to PRAK activation during endothelial cell migration, we examined the effects of a MEK1/2 inhibitor, PD98053, and a p38 inhibitor, SB203580, and shRNA for p38α or ERK3/4. As expected, SB203580 and PD98053 inhibited the tumor supernatant- and VEGF-induced kinase activity of p38 and ERK1/2, respectively, without affecting the other MAPK (Fig. 6D). The induction of PRAK kinase activity and T182 phosphorylation by tumor-secreted factors was disrupted only by SB203580 and not by PD98053 (Fig. 6D). In addition, shRNA for p38α, but not those for ERK3 or ERK4, inhibited the induction of activating phosphorylation of PRAK (Fig. 6F, 7A and 7B). Therefore, PRAK is activated by p38, but not by ERK1/2 or ERK3/4, during endothelial cell migration.

Consistent with the essential role of the p38-PRAK circuit in endothelial cell migration, SB203580 and p38α shRNA abolished the migration of HUVECs in response to skin tumor-secreted factors (Fig. 6E and G). PD98053 and another MEK inhibitor, U0126, also disrupted HUVEC migration (Fig. 6D), suggesting that the MEK-ERK pathway also contributes to endothelial cell migration, but likely via a PRAK-independent mechanism. The latter finding is consistent with previous reports that ERK2 regulates the dynamics of focal contacts in migrating cells by directly phosphorylating FAK and paxillin (21, 22, 27). None of the compounds had significant effects on the proliferation of HUVECs in the presence or absence of skin tumor supernatant (data not shown), indicating that inhibition of these pathways specifically altered the migration, but not the proliferation, of the endothelial cells. In contrast to what was seen for p38 and ERK1/2, knockdown of ERK3 or ERK4 had no effect on migration (Fig. 7D) of HUVECs, although ERK4 shRNAs inhibited their proliferation (Fig. 7C). Therefore, ERK3/4 are not required for either PRAK activation or HUVEC migration in response to tumor-secreted proangiogenic factors.

PRAK is essential for the activation of FAK on focal contacts and cytoskeletal reorganization during endothelial cell migration. To investigate the mechanism underlying the role of PRAK in endothelial cell migration, we analyzed the effect of PRAK deficiency on cytoskeletal reorganization, a crucial step in cell movement. Treatment with tumor supernatant or VEGF induced the formation of actin stress fibers crossing the cell in control HUVECs but not in cells with PRAK knockdown (Fig. 8A and B). Focal adhesion kinase (FAK) is a major regulator of

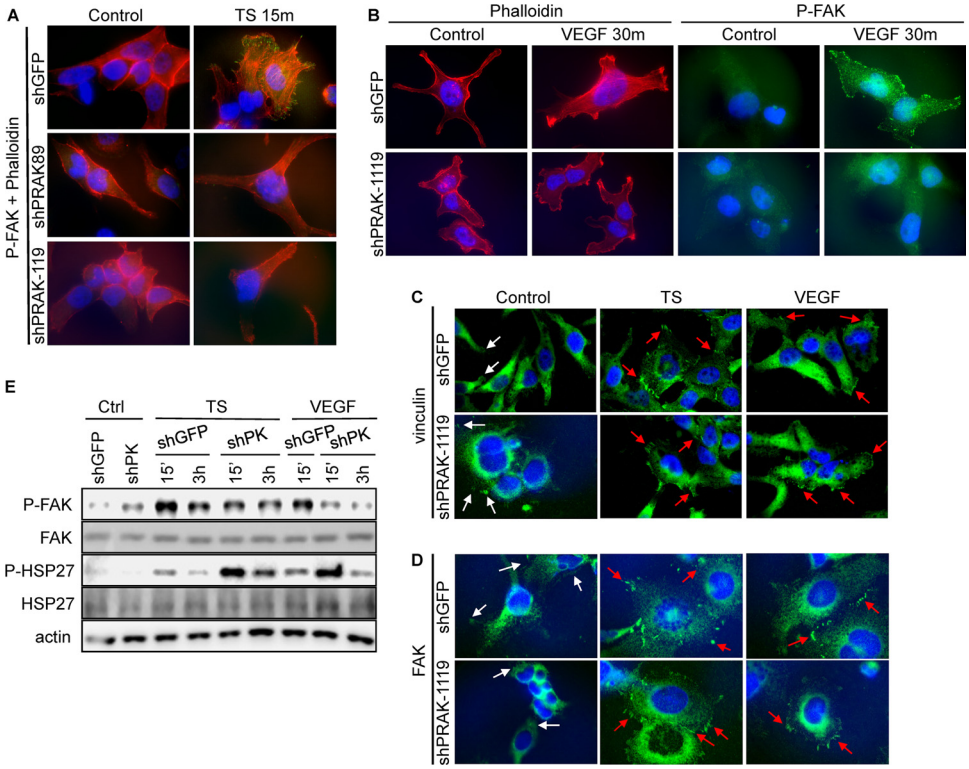

FIG 8 PRAK is essential for cytoskeletal reorganization and FAK activation by skin tumor-secreted proangiogenic factors. (A and B) HUVECs transduced with shRNA for GFP (shGFP) or PRAK (shPRAK89 and shPRAK1119) were treated with control medium (Control), tumor supernatant (TS) (A) or VEGF (B) for 15 min (A) or 30 min (B). Cells were stained with an anti-phospho-FAK (Y397) antibody (A) and/or (B) rhodamine-conjugated phalloidin. Activated FAK in focal contacts, actin filaments, and nuclei are shown in green, red, and blue, respectively. (C and D) HUVECs transduced with shRNA for GFP (shGFP) or PRAK (shPRAK1119) were treated with control medium (Control), tumor supernatant (TS), or VEGF for 30 min. Cells were stained with an antivinculin (C) or anti-FAK (D) antibody. FAK and vinculin signals and nuclei are shown in green and blue, respectively. Symbols: white arrows, small and sparse focal adhesions in control cells; red arrows, more-intensive focal adhesions induced by proangiogenic factors. (E) Western blot analysis of HUVECs transduced with shRNA for GFP (shGFP) or PRAK (shPK) and treated with control medium (Ctrl), tumor supernatant (TS), or VEGF for the indicated times.

cytoskeletal organization (30). In response to migratory stimuli, FAK is activated through phosphorylation on residues including Y397 and localized to focal contacts. We found that in control, unstimulated cells, the phospho-FAK-Y397 signal was weak, diffuse, and predominantly cytoplasmic. Treatment with tumor supernatant or VEGF induced a striking increase in phospho-FAK staining on focal adhesions and in the number of phospho-FAK-positive focal adhesions in control HUVECs but not in HUVECs expressing PRAK shRNA (Fig. 8A and B). Consistent with previous reports (1, 9), while small and sparse FAK- and vinculin-containing focal adhesions were present in untreated HUVECs, they were induced in both size and quantity by the skin tumor supernatant or VEGF, and PRAK knockdown did not alter the induction of these focal adhesions (Fig. 8C and D). Moreover, Western blot analysis revealed that PRAK silencing led to reduction in the steady-state level of activated FAK in cells but had no effect on the total level of FAK protein (Fig. 8E). Thus, PRAK is essential for FAK activation on focal contacts and cytoskeletal reorganization during migration of endothelial cells but is dispensable for the induction of focal adhesions and the expression and focal adhesion-localization of FAK.

The PRAK-FAK circuit mediates endothelial cell migration independently of the MK2-HSP27 pathway. MK2 is another p38 downstream substrate protein kinase related to PRAK (42). When activated by VEGF, MK2 regulates endothelial cell migration by phosphorylating and inactivating heat shock protein 27 (HSP27), an inhibitor of actin polymerization (15, 26, 39). Knockdown of MK2 (Fig. 6A and 9A) blocked tumor supernatant- and VEGF-induced HUVEC migration (Fig. 9B) and HSP27 phosphorylation (Fig. 9C) but not FAK activation (Fig. 9C). On the other hand, although PRAK can also phosphorylate HSP27 *in vitro*, VEGF- and skin tumor supernatant-induced HSP27 phosphorylation was intact in HUVECs expressing PRAK shRNA (Fig. 8E). Thus, PRAK and MK2 both contribute to endothelial cell migration by regulating different signaling events (activation of FAK and inactivation of HSP27, respectively) that are essential for cell motility.

PRAK and FAK are activated by tumor secreted proangiogenic factors via VEGFR2 during endothelial cell migration. VEGF-induced angiogenesis involves 3 VEGF receptors (VEGFR1 to -3) and 2 coreceptors (NRP1 and -2) (28). Despite the obvious expression of the other VEGF receptors in MVEC and HUVECs (Fig. 8A), we failed to detect VEGFR3 in these cells, possibly reflecting its restricted expression in lymphatic endothelium in adults (3). To examine the role of VEGF receptors in the activation of the PRAK-FAK circuit, we designed shRNA that effectively knocked down VEGFR1, VEGFR2,

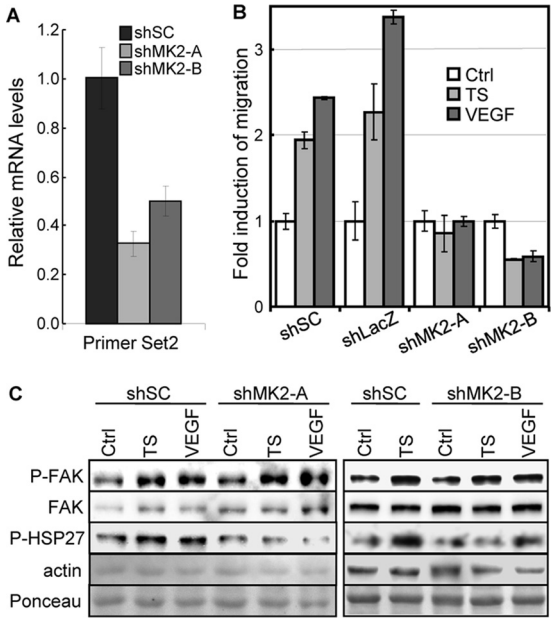

FIG 9 MK2 is essential for skin tumor supernatant- and VEGF-induced HUVEC migration and HSP27 phosphorylation but not for the activation of FAK. (A) Quantitative real-time PCR analysis of HUVECs transduced with a scrambled shRNA (shSC) or shRNA for MK2 (shMK2-A and -B), showing knockdown of MK2 by shRNA. (B) Migration activity of HUVECs transduced with a scrambled shRNA (shSC) or shRNA for LacZ (shLacZ) or MK2 (shMK2-A and -B) in response to control medium (Ctrl), skin tumor supernatant (TS), or 20 ng/ml of recombinant VEGF was measured in the Boyden chamber assay. The number of cells that had migrated to the bottom surface of the membrane among 1×10^4 seeded cells was counted in 10 randomly chosen 40× fields. The fold increase in migration was calculated for each cell line by dividing the average number of cells/field in the presence of TS or VEGF by that without stimuli (Ctrl). (A and B) All the numbers are mean ± SD for triplicates. (C) Western blot analysis of HUVECs transduced with a scrambled shRNA (shSC) or shRNA for MK2 (shMK2-A and -B) and treated with control medium (Ctrl), skin tumor supernatant (TS), or 20 ng/ml of recombinant VEGF for 30 min, detecting indicated proteins.

NRP1, or NRP2 (Fig. 10A). Silencing of VEGFR1, VEGFR2, and NRP1, but not of NRP2, led to the inhibition of the tumor supernatant- and VEGF-induced migration of HUVECs (Fig. 10B). Furthermore, the activation of PRAK and FAK was disrupted only by the VEGFR2 shRNA and not by shRNA for the other VEGF receptors (Fig. 10C). Therefore, while multiple VEGF receptors are essential for endothelial cell migration induced by skin tumor-secreted proangiogenic factors, the activation of PRAK and FAK is predominantly mediated by VEGFR2.

DISCUSSION

Combined with our previous report (45), the current study indicates that p38-PRAK pathway can either suppress or promote cancer development, depending on the stimulus of activation, the tissue type in which this pathway is activated, and the stage of carcinogenesis at which it is activated. When activated by oncogenes in normal skin epithelial cells, it suppresses tumor formation by triggering senescence. However, once senescence is compromised and tumors are formed, this pathway is activated by tumor-secreted proangiogenic factors in the host endothelial cells, resulting in migration of the endothelial cells and tumor angiogenesis supporting tumor growth and malignant progression. These findings have thus defined the temporal and spatial differences between the two opposite functions of the p38-PRAK pathway in cancer development in an *in vivo* model.

This study reveals a novel signaling pathway mediating the migration of host endothelial cells toward tumors and tumor angiogenesis, involving VEGF, VEGFR2, p38, PRAK, and FAK. Our results are consistent with the notion that tumor angiogenesis is a complicated process involving multiple parallel pathways. The p38-PRAK-FAK pathway identified in this study is novel and independent of the previously characterized p38-MK2-HSP27 pathway. Although PRAK and MK2 are both p38 downstream substrate kinases, their functions in cell migration diverge upon activation by p38 in response to proangiogenic factors. While PRAK is responsible for the activation of FAK but not the inactivation of HSP27, MK2 mediates the inactivation of HSP27 but not the activation of FAK. It has been documented that the MK2-HSP27 circuit mediates actin polymerization, a process that does not rely on FAK activation (38). Moreover, ERK1/2 are required only for cell migration and not for PRAK activation and thus are likely to contribute to cell motility by regulating pathways independent of PRAK and/or FAK. Besides p38 and ERK1/2, the atypical MAPKs ERK3 and ERK4 have also been implicated as upstream activators of PRAK (40, 41). However, although we cannot completely rule out their involvement, our data suggest that ERK3/4 may not be the major mediator of PRAK activation or HUVEC migration in response to skin tumor-secreted proangiogenic factors.

In this study, an autophosphorylation site Y397 was used to monitor FAK activation, which cannot be a direct PRAK substrate. FAK activity is regulated by multiple mechanisms (30), including phosphorylation by Src, dephosphorylation by protein tyrosine phosphatases, and interactions with positive and negative regulators. In addition, the FERM domain of FAK autoinhibits FAK activity by binding in *trans* to the FAK catalytic domain. PRAK may induce FAK by activating FAK kinases or other activators or by inactivating FAK inhibitors. Alternatively, PRAK may directly phosphorylate certain Ser/Thr residues on FAK, rendering FAK more accessible to its direct activators or relieving the inhibition by its negative regulators.

Angiogenesis is essential for both physiological and pathological processes (7, 37). Although the PRAK knockout mice are defective in tumor-induced angiogenesis, they display no deficiency in normal angiogenesis during development and have the same life span as their $PRAK^{+/+}$ and $PRAK^{+/-}$ littermates. These facts suggest that physiological angiogenesis and tumor angiogenesis are regulated by overlapping but distinct mechanisms and that the PRAK-mediated pathway is either inactive or functionally redundant with another pathway during developmental and physiological angiogenesis. There are precedents for such proteins required specifically for tumor angiogenesis. For example, the combination of heterozygous deletion of Id1 and homozygous deletion of Id3 ($Id1^{+/-}$ $Id3^{-/-}$), 2 genes encoding inhibitors for binding of basic helix-loop-helix (bHLH) transcription factors to DNA, leads to defects in tumor angiogenesis and impaired tumor growth, without affecting normal angiogenesis or the general health of the mice (29).

Our findings suggest that the p38-PRAK pathway may serve as

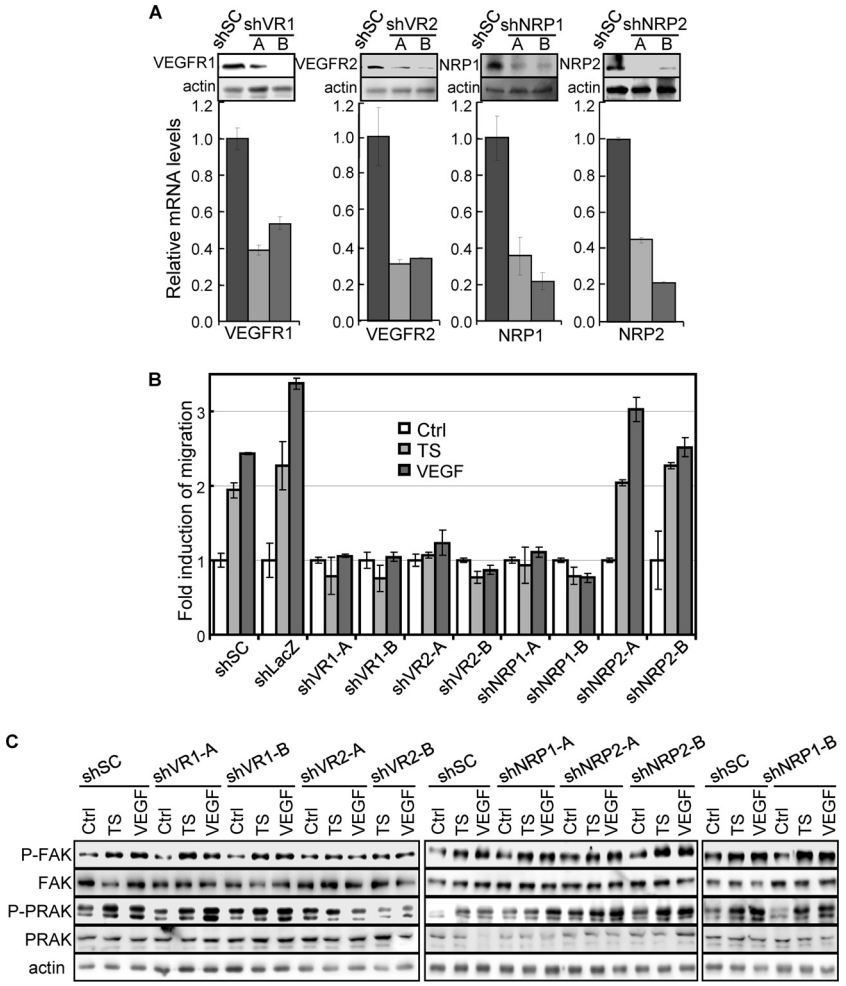

FIG 10 PRAK and FAK are activated by a VEGFR2-dependent pathway in response to skin tumor-secreted proangiogenic factors. (A) Quantitative real-time PCR (bottom bar graphs) and Western blot (top) analyses of HUVECs transduced with a scrambled shRNA sequence (shSC) or shRNA for VEGFR1 (shVR1-A and -B), VEGFR2 (shVR2-A and -B), NRP1 (shNRP1-A and -B), or NRP2 (shNRP2-A and -B), showing knockdown of targeted genes. Numbers in bar graphs are mean ± SD for triplicates after normalization to GAPDH signals. (B) Migration activity of HUVECs transduced with scrambled shRNA (shSC) or shRNA for VEGFR1 (shVR1-A and -B), VEGFR2 (shVR2-A and -B), NRP1 (shNRP1-A and -B), or NRP2 (shNRP2-A and -B) induced by control medium (Ctrl), skin tumor supernatant (TS), or 20 ng/ml of VEGF were measured in the Boyden chamber assay. The number of cells that had migrated to the bottom surface of the membrane among 1×10^4 seeded cells was counted in 10 randomly chosen 40× fields. The fold increase in migration was calculated for each cell line by dividing the average number of cells/field in the presence of TS or VG by that without stimuli (Con). All the numbers are mean ± SD for triplicates. (C) HUVEC lines described in panel B were subjected to Western blot analysis detecting indicated proteins.

an important new target for the antiangiogenic therapy of cancer. The requirement of PRAK in both skin carcinogenesis and LLC models suggests that it may play a key role in angiogenesis in multiple types of solid tumors. Since PRAK is essential for tumor angiogenesis and growth but not for normal angiogenesis and development, inhibitors of PRAK or other components of this pathway might be useful as specific antiangiogenic drugs for cancer. However, since the p38-PRAK pathway also contributes to the suppression of tumor formation in tissues such as skin epithelium, it may be necessary to deliver these inhibitors specifically into the host endothelial cells and/or to use these inhibitors for the treatment of cancer patients at advanced stages.

ACKNOWLEDGMENTS

This work was supported by grants from NIH (CA106768, CA131231, and RR025744 to P.S.) and NSF in China (30828019 to P.S. and J.H. and 91029304 to J.H.).

REFERENCES

1. **Abedi H, Zachary I.** 1997. Vascular endothelial growth factor stimulates tyrosine phosphorylation and recruitment to new focal adhesions of focal adhesion kinase and paxillin in endothelial cells. J. Biol. Chem. **272**: 15442–15451.
2. **Ambrosino C, Nebreda AR.** 2001. Cell cycle regulation by p38 MAP kinases. Biol. Cell **93**:47–51.
3. **Bahram F, Claesson-Welsh L.** 2010. VEGF-mediated signal transduction in lymphatic endothelial cells. Pathophysiology **17**:253–261.
4. **Brantley-Sieders DM, et al.** 2005. Impaired tumor microenvironment in EphA2-deficient mice inhibits tumor angiogenesis and metastatic progression. FASEB J. **19**:1884–1886.
5. **Bulavin DV, et al.** 2001. Initiation of a G2/M checkpoint after ultraviolet radiation requires p38 kinase. Nature **411**:102–107.
6. **Bulavin DV, Kovalsky O, Hollander MC, Fornace AJ, Jr.** 2003. Loss of oncogenic H-ras-induced cell cycle arrest and p38 mitogen-activated protein kinase activation by disruption of Gadd45a. Mol. Cell. Biol. **23**:3859–3871.
7. **Carmeliet P, Jain RK.** 2000. Angiogenesis in cancer and other diseases. Nature **407**:249–257.

8. **Cazillis M, et al.** 2004. Disruption of MKK4 signaling reveals its tumor-suppressor role in embryonic stem cells. Oncogene **23**:4735–4744.
9. **Cezar-de-Mello PF, Nascimento-Silva V, Villela CG, Fierro IM.** 2006. Aspirin-triggered Lipoxin A4 inhibition of VEGF-induced endothelial cell migration involves actin polymerization and focal adhesion assembly. Oncogene **25**:122–129.
10. **DeBusk LM, Massion PP, Lin PC.** 2008. IkappaB kinase-alpha regulates endothelial cell motility and tumor angiogenesis. Cancer Res. **68**:10223–10228.
11. **DiGiovanni J.** 1991. Modification of multistage skin carcinogenesis in mice. Prog. Exp. Tumor Res. **33**:192–229.
12. **DiGiovanni J.** 1992. Multistage carcinogenesis in mouse skin. Pharmacol. Ther. **54**:63–128.
13. **Faust D, et al.** 2005. p38alpha MAPK is required for contact inhibition. Oncogene **24**:7941–7945.
14. **Folkman J.** 1995. Angiogenesis in cancer, vascular, rheumatoid and other disease. Nat. Med. **1**:27–31.
15. **Guay J, et al.** 1997. Regulation of actin filament dynamics by p38 map kinase-mediated phosphorylation of heat shock protein 27. J. Cell Sci. **110**:357–368.
16. **Han J, Sun P.** 2007. The pathways to tumor suppression via route p38. Trends Biochem. Sci. **32**:364–371.
17. **Haq R, et al.** 2002. Constitutive p38HOG mitogen-activated protein kinase activation induces permanent cell cycle arrest and senescence. Cancer Res. **62**:5076–5082.
18. **Hirose Y, et al.** 2003. The p38 mitogen-activated protein kinase pathway links the DNA mismatch repair system to the G2 checkpoint and to resistance to chemotherapeutic DNA-methylating agents. Mol. Cell. Biol. **23**: 8306–8315.
19. **Hsieh YH, et al.** 2007. p38 mitogen-activated protein kinase pathway is involved in protein kinase Calpha-regulated invasion in human hepatocellular carcinoma cells. Cancer Res. **67**:4320–4327.
20. **Hui L, et al.** 2007. p38alpha suppresses normal and cancer cell proliferation by antagonizing the JNK-c-Jun pathway. Nat. Genet. **39**:741–749.
21. **Hunger-Glaser I, Fan RS, Perez-Salazar E, Rozengurt E.** 2004. PDGF and FGF induce focal adhesion kinase (FAK) phosphorylation at Ser-910: dissociation from Tyr-397 phosphorylation and requirement for ERK activation. J. Cell Physiol. **200**:213–222.
22. **Ishibe S, Joly D, Zhu X, Cantley LG.** 2003. Phosphorylation-dependent paxillin-ERK association mediates hepatocyte growth factor-stimulated epithelial morphogenesis. Mol. Cell **12**:1275–1285.
23. **Iwasa H, Han J, Ishikawa F.** 2003. Mitogen-activated protein kinase p38 defines the common senescence-signalling pathway. Genes Cells **8**:131–144.
24. **Kwong J, et al.** 2009. p38alpha and p38gamma mediate oncogenic ras-induced senescence through differential mechanisms. J. Biol. Chem. **284**: 11237–11246.
25. **Lamalice L, Houle F, Jourdan G, Huot J.** 2004. Phosphorylation of tyrosine 1214 on VEGFR2 is required for VEGF-induced activation of Cdc42 upstream of SAPK2/p38. Oncogene **23**:434–445.
26. **Landry J, Huot J.** 1999. Regulation of actin dynamics by stress-activated protein kinase 2 (SAPK2)-dependent phosphorylation of heat-shock protein of 27 kDa (Hsp27). Biochem. Soc. Symp. **64**:79–89.
27. **Liu ZX, Yu CF, Nickel C, Thomas S, Cantley LG.** 2002. Hepatocyte growth factor induces ERK-dependent paxillin phosphorylation and regulates paxillin-focal adhesion kinase association. J. Biol. Chem. **277**: 10452–10458.
28. **Lohela M, Bry M, Tammela T, Alitalo K.** 2009. VEGFs and receptors involved in angiogenesis versus lymphangiogenesis. Curr. Opin. Cell Biol. **21**:154–165.
29. **Lyden D, et al.** 1999. Id1 and Id3 are required for neurogenesis, angiogenesis and vascularization of tumour xenografts. Nature **401**:670–677.
30. **Mitra SK, Hanson DA, Schlaepfer DD.** 2005. Focal adhesion kinase: in command and control of cell motility. Nat. Rev. Mol. Cell Biol. **6**:56–68.
31. **Nebreda AR, Porras A.** 2000. p38 MAP kinases: beyond the stress response. Trends Biochem. Sci. **25**:257–260.
32. **New L, Jiang Y, Han J.** 2003. Regulation of PRAK subcellular location by p38 MAP kinases. Mol. Biol. Cell **14**:2603–2616.
33. **New L, et al.** 1998. PRAK, a novel protein kinase regulated by the p38 MAP kinase. EMBO J. **17**:3372–3384.
34. **Ni H, Wang XS, Diener K, Yao Z.** 1998. MAPKAPK5, a novel mitogen-activated protein kinase (MAPK)-activated protein kinase, is a substrate of the extracellular-regulated kinase (ERK) and p38 kinase. Biochem. Biophys. Res. Commun. **243**:492–496.
35. **Ono K, Han J.** 2000. The p38 signal transduction pathway: activation and function. Cell. Signal. **12**:1–13.
36. **Raman M, Earnest S, Zhang K, Zhao Y, Cobb MH.** 2007. TAO kinases mediate activation of p38 in response to DNA damage. EMBO J. **26**:2005–2014.
37. **Risau W.** 1997. Mechanisms of angiogenesis. Nature **386**:671–674.
38. **Rousseau S, et al.** 2000. Vascular endothelial growth factor (VEGF)-driven actin-based motility is mediated by VEGFR2 and requires concerted activation of stress-activated protein kinase 2 (SAPK2/p38) and geldanamycin-sensitive phosphorylation of focal adhesion kinase. J. Biol. Chem. **275**:10661–10672.
39. **Rousseau S, Houle F, Landry J, Huot J.** 1997. p38 MAP kinase activation by vascular endothelial growth factor mediates actin reorganization and cell migration in human endothelial cells. Oncogene **15**:2169–2177.
40. **Schumacher S, et al.** 2004. Scaffolding by ERK3 regulates MK5 in development. EMBO J. **23**:4770–4779.
41. **Seternes OM, et al.** 2004. Activation of MK5/PRAK by the atypical MAP kinase ERK3 defines a novel signal transduction pathway. EMBO J. **23**: 4780–4791.
42. **Shi Y, Gaestel M.** 2002. In the cellular garden of forking paths: how p38 MAPKs signal for downstream assistance. Biol. Chem. **383**:1519–1536.
43. **Shin I, Kim S, Song H, Kim HR, Moon A.** 2005. H-Ras-specific activation of Rac-MKK3/6-p38 pathway: its critical role in invasion and migration of breast epithelial cells. J. Biol. Chem. **280**:14675–14683.
44. **Sodhi A, et al.** 2000. The Kaposi's sarcoma-associated herpes virus G protein-coupled receptor up-regulates vascular endothelial growth factor expression and secretion through mitogen-activated protein kinase and p38 pathways acting on hypoxia-inducible factor 1alpha. Cancer Res. **60**: 4873–4880.
45. **Sun P, et al.** 2007. PRAK is essential for ras-induced senescence and tumor suppression. Cell **128**:295–308.
46. **Vanderkerken K, et al.** 2007. Inhibition of p38alpha mitogen-activated protein kinase prevents the development of osteolytic bone disease, reduces tumor burden, and increases survival in murine models of multiple myeloma. Cancer Res. **67**:4572–4577.
47. **Ventura JJ, et al.** 2007. p38alpha MAP kinase is essential in lung stem and progenitor cell proliferation and differentiation. Nat. Genet. **39**:750–758.
48. **Wang W, et al.** 2002. Sequential activation of the MEK-extracellular signal-regulated kinase and MKK3/6-p38 mitogen-activated protein kinase pathways mediates oncogenic ras-induced premature senescence. Mol. Cell. Biol. **22**:3389–3403.
49. **Wu CC, Wu X, Han J, Sun P.** 2010. p38gamma regulates UV-induced checkpoint signaling and repair of UV-induced DNA damage. Protein Cell **1**:573–583.
50. **Yamaguchi T, et al.** 2008. Development of a new method for isolation and long-term culture of organ-specific blood vascular and lymphatic endothelial cells of the mouse. FEBS J. **275**:1988–1998.
51. **Yoshino Y, et al.** 2006. Activation of p38 MAPK and/or JNK contributes to increased levels of VEGF secretion in human malignant glioma cells. Int. J. Oncol. **29**:981–987.